

# The Homology and Phylogeny of Chondrichthyan Tooth Enameloid

J. Andrew Gillis\* and Philip C.J. Donoghue

Department of Earth Sciences, University of Bristol, Bristol, BS8 1RJ, UK

**ABSTRACT** A systematic SEM survey of tooth microstructure in (primarily) fossil taxa spanning chondrichthyan phylogeny demonstrates the presence of a superficial cap of single crystallite enameloid (SCE) on the teeth of several basal elasmobranchs, as well as on the tooth plates of *Helodus* (a basal holocephalan). This suggests that the epithelial–mesenchymal interactions required for the development of enameloid during odontogenesis are plesiomorphic in chondrichthyans, and most likely in toothed gnathostomes, and provides phylogenetic support for the homology of chondrichthyan and actinopterygian enameloid. Along the neoselachian stem, we see a crownward progression, possibly modulated by heterochrony, from a monolayer of SCE lacking microstructural differentiation to the complex triple-layered tooth enameloid fabric of neoselachians. Finally, the occurrence of fully-differentiated neoselachian enameloid microstructure (including compression-resistant tangle fibered enameloid and bending-resistant parallel fibered enameloid) in *Chlamydoselachus anguineus*, a basal Squalean with teeth that are functionally “cladodont,” is evidence that triple-layered enameloid microstructure was a pre-adaptation to the cutting and gouging function of many neoselachian teeth, and thus may have played an integral role in the Mesozoic radiation of the neoselachian crown group. *J. Morphol.* 268:33–49, 2007. © 2006 Wiley-Liss, Inc.

**KEY WORDS:** Chondrichthyes; enameloid microstructure; tooth homology; paleohistology

The teeth of chondrichthyans and actinopterygians are both capped with enameloid—a hypermineralized tissue with a matrix of mixed ameloblastic (ectodermal) and odontoblastic (ectomesenchymal) origin (Shellis and Miles, 1974, 1976; Smith and Hall, 1990; Sasagawa, 1999). While broad developmental and histological similarities between the tissues in the two taxa have led some to argue for their homology (Moss, 1977), subtle differences in organic composition and mineralization patterns between chondrichthyan and actinopterygian enameloid (Sasagawa, 2002), as well as the purported absence of enameloid on the teeth of basal elasmobranchs (Øvig, 1966; Gross, 1973), have led others to speculate that these tissues may, instead, be the products of convergent evolution (Bendix-Almgreen, 1983; Sasagawa, 2002). Indeed, this view accords with recent suggestions that, far from being a shared primitive character of jawed vertebrates, teeth have evolved independently among chondrichthyans and

osteichthyans (Smith, 2003; Johanson and Smith, 2003; Smith and Johanson, 2003) and, thus, scenarios in which teeth and jaws are the key innovations underpinning an adaptive radiation of jawed vertebrates may be entirely unfounded.

A comprehensive survey of tooth microstructure in chondrichthyans would undoubtedly clarify the phylogenetic relationship between chondrichthyan and actinopterygian enameloid (Moss, 1977; Bendix-Almgreen, 1983; Sasagawa, 2002). The primitive actinopterygian condition is already well established (Janvier, 1978; Smith, 1992; Richter and Smith, 1995). However, to date, studies of chondrichthyan enameloid microstructure have focused almost exclusively on crown neoselachians (defined herein as the clade of fossil and living taxa derived from the last common ancestor of living neoselachians), (Ripa et al., 1972; Reif, 1973, 1977, 1979; Duffin, 1980; Thies, 1982; Iwai-Liao et al., 1992; Cuny et al., 1998), or on Mesozoic Hybodontiformes (e.g. Cuny et al., 2001). Virtually no data are available on enameloid microstructure in the teeth of the diverse non-neoselachian chondrichthyans (Fig. 6) and, thus, the condition of the last common ancestor of chondrichthyans and actinopterygians is unknown. Within this context, debate over homology of chondrichthyan and actinopterygian enameloid must similarly be considered unresolved.

The dearth of available data on non-neoselachian chondrichthyans also impacts upon our understanding of how the microstructural differentiation of tooth enameloid, so characteristic of neoselachians (Reif, 1973, 1977, 1979), was achieved. At present, microstructural differentiation is thought to be one of the key adaptive innovations facilitating novel feeding strategies among neoselachians (Thies and Reif, 1985) through functional adaptation to force resistance during cutting and gouging predation

---

Contract grant sponsor: Palaeontological Association.

\*Correspondence to: J. Andrew Gillis, Department of Organismal Biology and Anatomy, University of Chicago, 1027 E, 57th Street, Chicago, IL 60637. E-mail: jagillis@uchicago.edu

Published online 4 December 2006 in  
Wiley InterScience (www.interscience.wiley.com)  
DOI: 10.1002/jmor.10501

(Preuschoft et al., 1974; Reif, 1978, 1979; Thies and Reif, 1985). However, the precise nature of this structure–function relationship has never been examined in a phylogenetic context.

We have attempted to resolve these issues through scanning electron microscopic examination of ground tooth sections from a variety of chondrichthyan taxa (primarily non-neoselachian chondrichthyans with clutching and grasping teeth, though *Chlamydoselachus anguineus*, a basal neoselachian, and *Helodus*, a stem holocephalan, were also examined), and these data were analyzed within a phylogenetic framework. As the taxonomic composition of the Elasmobranchii varies considerably among the phylogenetic hypotheses considered, chondrichthyans will herein be classified as stem or crown group holocephalans, crown group neoselachians, or “non-neoselachians” (a necessarily awkward grouping of all “sharks” that are not members of the crown group Neoselachii, and that may, or may not, lie along the neoselachian stem). Data were interpreted in light of several alternative (and often conflicting) published phylogenies. All non-neoselachian teeth examined (with the exception of certain Xenacanthiformes), as well as the tooth plates of *Helodus*, are revealed to possess a layer of hypermineralized single crystallite enameloid (SCE, i.e. an enameloid monolayer composed of randomly oriented single crystallites) with no apparent microstructural differentiation. By inference, tooth enameloid is a plesiomorphy of chondrichthyans and, therefore, of toothed gnathostomes. *Chlamydoselachus anguineus* possesses the fully differentiated triple-layered enameloid fabric typical of crown neoselachians, and it therefore appears that chondrichthyan tooth enameloid underwent a rapid and complex microstructural reorganization near the base of the radiation of crown neoselachians. Furthermore, the presence of fully differentiated three-layered enameloid in *C. anguineus*, a basal neoselachian with clutching and grasping teeth, as well as reports of this microstructure in the front grasping teeth of *Heterodontus* (Reif, 1977), suggest that this enameloid microstructure was, in fact, a preadaptation to the cutting and gouging function of many neoselachian teeth (as implied in Preuschoft et al., 1974). Finally, evidence of significant changes to the organization of the enameloid matrix among non-neoselachians, as well as commonality of enameloid microstructure to stem-actinopterygians, is suggestive of homology, and not convergence, of enameloid—and indeed, teeth—among early jawed vertebrates.

## MATERIALS AND METHODS

### Chondrichthyan Taxa Examined

Three crown neoselachian taxa—*Carcharhinus plumbeus*, *Carcharias* sp., and *Chlamydoselachus anguineus*—were examined in this study. Teeth of the brown shark (*C. plumbeus*, recent—BRSUG 27191, Bristol University Geological Museum, Bristol,

UK) were obtained from the London Aquarium, and fossil *Carcharias* sp. teeth (BRSUG 27192) from the Cretaceous of Morocco were obtained from a private collector. Frilled shark (*C. anguineus*) teeth were dissected from the jaw of a recent specimen (AMNH 13813, American Museum of Natural History, New York, NY) caught off the coast of Japan.

The non-neoselachian taxa examined in this study may be broadly grouped into orders/superorders based loosely on the classification scheme of Cappetta et al. (1993). Teeth from two tooth-based hybodontiform taxa—*Hybodus nebraskensis* and *Protacrodus serra*—were examined here. *Hybodus nebraskensis* (CM 44547, Carnegie Museum of Natural History, Pittsburgh, PA) teeth were recovered from Upper Pennsylvanian (Late Carboniferous) sediments of Peru, NE, while teeth of *P. serra* (BRSUG 27193) were collected from Upper Famennian (Late Devonian) limestone of the Tafilalt Platform, Morocco. Teeth of the ctenacanthiform sharks *Ctenacanthus compressus* (CMNH 9207, Cleveland Museum of Natural History, Cleveland, OH) and *Ctenacanthus* sp. (CMNH 5290), as well as teeth of a “cladodont” shark (CMNH 5121) and the cladoselachiform shark *Cladoseleche kepleri* (CMNH 5420), were collected from the Upper Devonian Cleveland Shale in Cleveland, OH. Teeth of the xenacanthiform sharks *Orthacanthus compressus* (CM 44556) and *Orthacanthus* sp. (AMNH 7115) were recovered from Upper Pennsylvanian sediments of Peru, NE, and Lower Permian sediments of Whiskey Creek, TX, respectively. Teeth of the phoebodontiform shark *Jalodus australiensis* (BRSUG 27194) were collected from Famennian sediments of the Ostrówka Quarry, Holy Cross Mountains, Poland, and teeth of the symmoriiform shark *Akmonistion zangerli* (UMZC GN.1047, University Museum of Zoology, Cambridge University, Cambridge, England) were recovered from the Namurian (Middle Carboniferous) Top Hosie Limestone of Bearsden, Scotland.

Tooth plates of the basal holocephalan *Helodus* sp. (BRSUG 27195) were collected from the Carboniferous Cromhall Limestone of South Gloucestershire, England.

### SEM Analysis of Enameloid Microstructure

Teeth that were only partially exposed were not prepared out, and were sectioned with any remaining matrix in place (to avoid damage to the enameloid layer). Teeth were embedded in transparent polyester resin (Struers.) prior to sectioning, and were cut in cross- or longitudinal section using a diamond lapidary blade (M.K. Diamond Products, 153742) on an Isomet low speed saw (Buehler). For an illustrated description of relevant planes of section, see Figure 1. Following the initial cut, the surface of the resin block to be observed was ground, until the desired plane of section was reached, using 800-, 1200-, 2400-, and 4000-grit silicon carbide abrasive paper. Ground sections were then polished on a polishing pad (Kemet, PSU-M) with 6 and 1  $\mu\text{m}$  Kemet diamond polish (and Kemet Type-W polishing lubricant), and etched for 5 or 10 s in 5 or 10% HCl.

Prior to SEM analysis, ground sections were coated with gold, and colloidal graphite (Agar Scientific, G303) was used to enhance electron conductivity between the specimen and the stub, and to minimize charging effects. Following an initial examination of the section under SEM, the gold coat was removed using a 0.25  $\mu\text{m}$  diamond polishing lap, and sections were ground further, repolished, etched, and coated. This was repeated as many times as was necessary to elucidate enameloid microstructure. Analysis and photography of ground sections was carried out on a Hitachi S-3500N scanning electron microscope in secondary electron mode, with an acceleration voltage of 20 or 25 kV.

## RESULTS

### Tooth Enameloid Microstructure

**The Neoselachii: *Carcharhinus plumbeus* and *Carcharias* sp.** The serrated teeth of the Brown Shark, *Carcharhinus plumbeus* (BRSUG

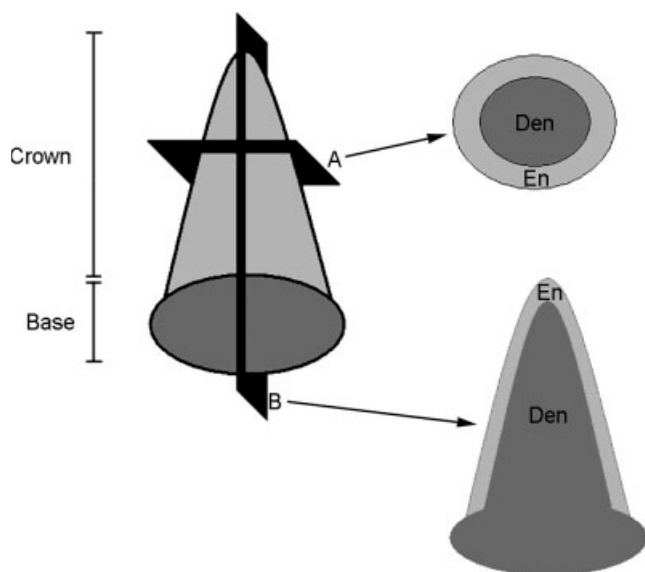


Fig. 1. Schematic diagram of a tooth illustrating histological planes of section, and relative spatial arrangements of relevant tissue types. (a) Cross section. (b) Longitudinal section. den, dentine; en, enameloid.

27191), exhibit the three-layered enameloid microstructure characteristic of the cutting and gouging teeth of neoselachian sharks. When examined in longitudinal section, the enameloid layer is organized into a series of regularly spaced superficial ridges (Fig. 2a) composed of parallel fibered enameloid (PFE, Fig. 2b). In this layer, individual hydroxyapatite crystallites are not discernable, as they are tightly arranged into thick fiber bundles (2–3  $\mu\text{m}$  in diameter) oriented normal to the outer enameloid surface, and extending from the outer enameloid surface to the basal layer of tangle fibered enameloid (TFE). Radial crystal bundles can also be seen throughout the PFE layer running parallel to the outer enameloid surface, and at  $90^\circ$  to the surface normal parallel bundles.

Beneath the PFE lies a layer of TFE (Fig. 2c), and the border between the two layers is clearly defined. Hydroxyapatite crystallites are, once again, organized into thick bundles, and individual crystallites are not discernable. Crystallite bundles in the TFE layer interweave, and are oriented roughly parallel to the outer enameloid surface and the enameloid–dentine junction. The outermost shiny layer enameloid (SLE, a thin layer of enameloid composed of randomly oriented single crystallites not arranged into bundles) is not present, though this is likely an artifact of etching (the sensitivity of SLE to etching during SEM preparation is noted and discussed in Reif, 1979).

In the fossilized teeth of *Carcharias* sp. (BRSUG 27192), a layer of PFE overlying basal TFE is, once again, present (Fig. 2d), as is an outer shiny layer of enameloid (Fig. 2e). In cross-section, the parallel

bundles of the PFE are evenly spaced and less densely packed, revealing abundant radial bundles (Fig. 2f). Crystallite bundles are 2–3  $\mu\text{m}$  in diameter. Beneath the PFE lies a layer of TFE (Fig. 2g), and, as in *Carcharhinus plumbeus*, a clear border exists between the two layers. Crystallite bundles in TFE interweave, and are oriented roughly parallel to the outer enameloid surface and the enameloid–dentine junction. A well-defined enameloid–dentine junction is present (Fig. 2d). The teeth of *Carcharias* sp. possess lateral cutting edges running down the entire length of each side of the primary cusp. These cutting edges possess a complex tangle-like enameloid microstructure that originates above the PFE layer (Fig. 2h).

***Chlamydoselachus anguineus*.** The tricuspid grasping teeth of the frilled shark, *Chlamydoselachus anguineus* (AMNH 13813), exhibit a fully differentiated three-layered enameloid microstructure, comparable to that observed in the neoselachians *Carcharhinus plumbeus* and *Carcharias* sp. (Fig. 2i). Cusps are round in cross-section, and possess lateral cutting edges running down opposite sides from the cusp tip to the base (Fig. 2j). The SLE has been etched away, but immediately beneath the outer enameloid surface is a layer of PFE (Fig. 2k). There are evenly spaced remains of outer enameloid surface-normal parallel crystallite bundles of  $\sim 2 \mu\text{m}$  in diameter, and abundant radial bundles.

The border between PFE and underlying TFE is not as striking in *Chlamydoselachus anguineus* as in *Carcharhinus plumbeus* and *Carcharias* sp., but is still reasonably perceptible. A layer of TFE lies between the PFE and the enameloid–dentine junction, and although etching has obscured the fibers somewhat, the tangled orientation of mineral bundles is clearly discernable, and is in sharp contrast to the orientation of bundles in the overlying layer of PFE (Fig. 2l). The cutting edges of the tooth cusp also originate above the layer of PFE, with no connection to the TFE lying between the PFE and the enameloid–dentine junction (Fig. 2m).

**Hybodontiformes: *Hybodus nebraskensis* and *Protacrodus serra*.** The ridged grasping teeth of *Hybodus nebraskensis* (CM 44547) possess a homogeneous layer of SCE that lacks any microstructural differentiation (Fig. 3a), and differs markedly from the highly porous dentine that underlies it (Fig. 3b). Individual enameloid crystallites (0.5–1  $\mu\text{m}$  in length) are discernable within the layer, and they appear to be randomly oriented (Fig. 3c). A clear border exists between the SCE layer and the underlying dentine, and remnants of odontoblast cell processes extend into the enameloid cap (Fig. 3a).

The teeth of the basal hybodontiform *Protacrodus serra* (BRSUG 27193) are also capped with a homogeneous ridged layer of SCE (Fig. 3d). Individual crystallites are visible, and demonstrate no preferred orientation (Fig. 3e). The remnants of onto-

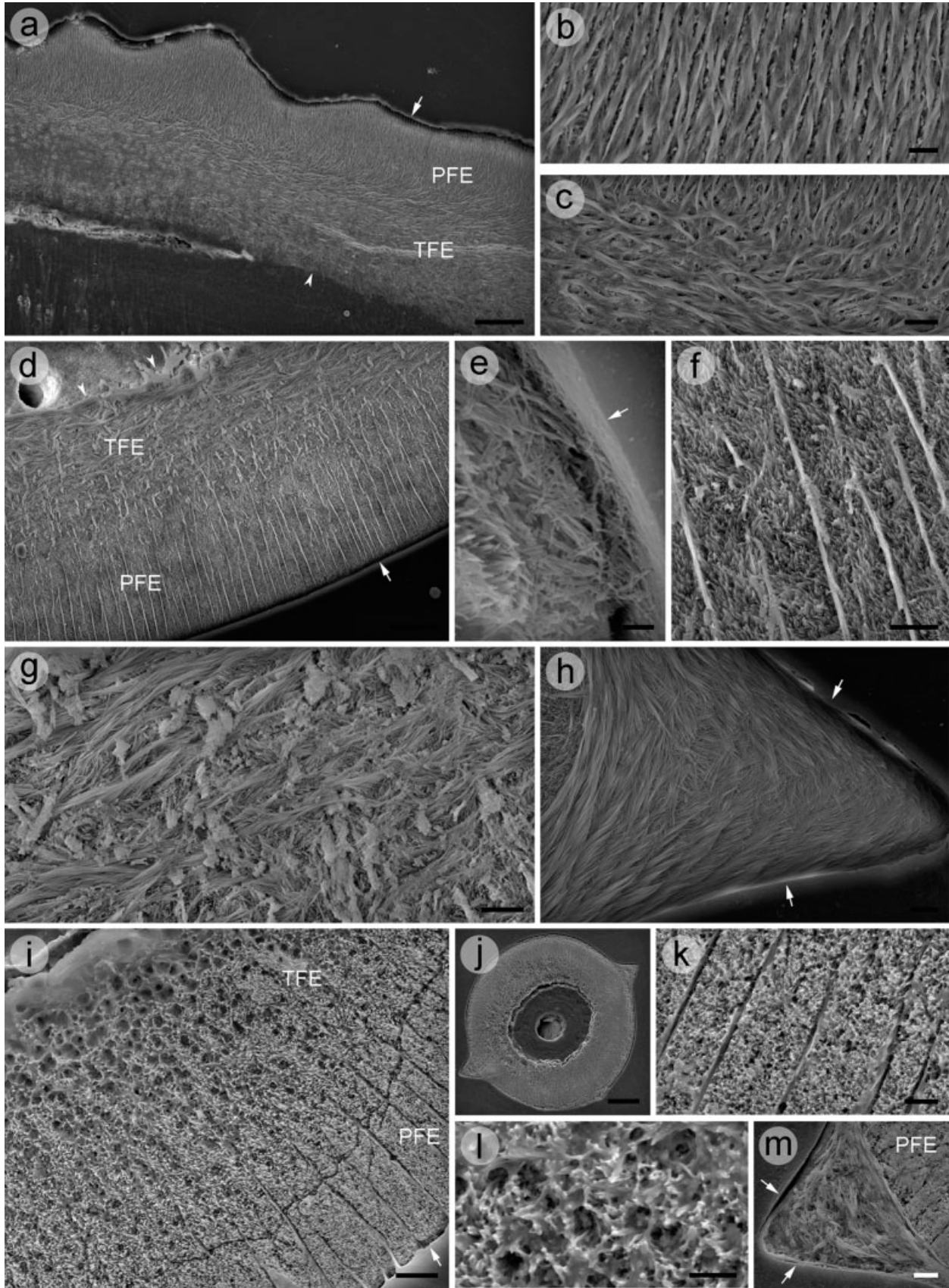


Figure 2

blast cell process canals can be seen at the base of the enameloid layer, and a well-defined border exists between the enameloid monolayer and the dentine core. The dentine core appears to be composed of orthodentine, deposited in concentric rings around an undivided central pulp canal.

**Ctenacanthiformes: *Ctenacanthus compressus* and *Ctenacanthus* sp.** The teeth of *Ctenacanthus compressus* (CMNH 9207) possess an enameloid cap that is organized into evenly spaced ridges, and is hypermineralized to such an extent that individual hydroxyapatite crystallites are not discernable (Fig. 3f). However, the enameloid layer is histologically distinguishable from the underlying osteodentine, as it clearly lacks the porous and tubule-rich texture of dentine matrix (Fig. 3g). Etching reveals no indication of any degree of microstructural differentiation within the enameloid layer, and thus the presence of a monolayer of SCE (comparable to that observed in Hybodontiformes) is inferred. A distinct border exists between the enameloid layer and the underlying dentine, and numerous odontoblast cell process canals can be seen extending across the enameloid–dentine junction into the enameloid cap (Fig. 3h).

The sharp contrast between a hypermineralized enameloid cap and underlying dentine is once again exemplified in the teeth *Ctenacanthus* sp. (CMNH 5290, Fig. 3i). In this specimen, a fossilized dentine core, composed of an outer layer of pallial orthodentine (exhibiting ruffled lines of incremental growth and remnants of abundant odontoblast cell processes) surrounding inner osteodentine with numerous denteons, is capped by an undifferentiated enameloid monolayer. Cell processes can be seen extending into the hypermineralized cap, though cell processes within the enameloid itself and individual enameloid crystallites are not discernable (Fig. 3j).

**Cleveland Shale “cladodont” shark.** The isolated tooth of an unidentified “cladodont” shark (CMNH 5121), from the Devonian Cleveland Shale, OH, was examined. Based on size and general morphology, this tooth was classified as belonging to either *Cladoselache* or *Ctenacanthus*, though the microstructure of the dentine core (a prominent cen-

ter composed of osteodentine with numerous denteons, surrounded by concentric rings of pallial orthodentine) bears a striking resemblance to that of *Ctenacanthus compressus* (CMNH 9207) and *Ctenacanthus* sp. (CMNH 5290), and differs considerably from the primarily orthodontinuous core of *Cladoselache kepleri* (CMNH 5420). In cross-section, a homogeneous monolayer of SCE is evident (Fig. 3k). The layer lies above a distinct enameloid–dentine junction, and odontoblast cell processes can be seen traversing the junction and extending into the enameloid. Examination of the enameloid monolayer under higher magnification reveals individual mineral crystallites elongate in morphology, that measure 0.5–1  $\mu\text{m}$  in length (Fig. 3l). No microstructural differentiation is observed across the layer, and the enameloid crystallites appear to be arranged randomly with no preferred orientation relative to the outer enameloid surface. The stark differentiation between the enameloid monolayer and dentine, the presence of a sharp enameloid–dentine junction, and the size/shape of component crystallites are all comparable to the condition in *Hybodus nebraskensis*. In addition, dentine microstructure is exceptionally well preserved in this cladodont tooth, confirming that there is little if any diagenetic alteration (Fig. 3m). Numerous concentric growth lines in the outer layer of pallial orthodentine, indicative of incremental deposition and mineralization, are discernable, and abundant tubules (derived from odontoblast cell processes) emanate from well-preserved denteons in the central core of osteodentine (Fig. 3m).

**Xenacanthiformes: *Orthacanthus compressus* and *Orthacanthus* sp.** The bicuspid grasping teeth of *Orthacanthus compressus* (CM 44556), viewed in longitudinal section, appear to lack an enameloid cap (Fig. 4a). The teeth are uniformly composed of concentrically deposited orthodentine with abundant odontoblast tubules originating from a central pulp canal, but no histologically distinct hypermineralized capping tissue is present (Fig. 4b). Conversely, the bicuspid teeth of *Orthacanthus* sp. (AMNH 7115) do appear to possess a cap of hypermineralized tissue resembling SCE. Viewed in cross-section, the capping tissue is unevenly distrib-

Fig. 2. Tooth enameloid microstructure of the neoselachian elasmobranchs *Carcharhinus plumbeus* (a–c), *Carcharias* sp. (d–h), and *Chlamydoselachus anguineus* (i–m). SEM (a) longitudinal section through the serrated enameloid layer of BRSUG 27191. Etched 5 s in 5% HCl. Scale bar = 100  $\mu\text{m}$ . (b) Detail of the PFE layer in a longitudinal section of BRSUG 27191. Etched 5 s in 5% HCl. Scale bar = 10  $\mu\text{m}$ . (c) TFE layer in a longitudinal section of BRSUG 27191. Etched 5 s in 5% HCl. Scale bar = 20  $\mu\text{m}$ . (d) Overview of the enameloid layer as seen in a cross-section through BRSUG 27192. Etched 5 s in 10% HCl. Scale bar = 40  $\mu\text{m}$ . (e) The SLE layer of BRSUG 27192, viewed in cross-section. Etched 5 s in 10% HCl. Scale bar = 2  $\mu\text{m}$ . (f) A cross-section through the PFE of BRSUG 27192. Etched 5 s in 10% HCl. Scale bar = 10  $\mu\text{m}$ . (g) The TFE layer of BRSUG 27192, viewed in cross-section. Etched 5 s in 10% HCl. Scale bar = 10  $\mu\text{m}$ . (h) Cross-section through the lateral cutting edges of BRSUG 27192. Etched 5 s in 10% HCl. Scale bar = 10  $\mu\text{m}$ . (i) A cross-section through the enameloid layer of AMNH 13813. Etched 5 s in 5% HCl. Scale bar = 10  $\mu\text{m}$ . (j) Overview of the cross-sectional tooth morphology of AMNH 13813. Etched 5 s in 5% HCl. Scale bar = 70  $\mu\text{m}$ . (k) A cross-section through the PFE of AMNH 13813. Etched 5 s in 5% HCl. Scale bar = 5  $\mu\text{m}$ . (l) Cross-section through the remnants of the basal TFE layer of AMNH 13813. Etched 5 s in 5% HCl. Scale bar = 4  $\mu\text{m}$ . (m) The lateral cutting edges of AMNH 13813, viewed in cross-section. Etched 5 s in 5% HCl. Scale bar = 7.5  $\mu\text{m}$ . Arrows denote the outer enameloid surface. Arrowheads denote the enameloid–dentine junction. PFE, parallel fibered enameloid; TFE, tangle fibered enameloid.

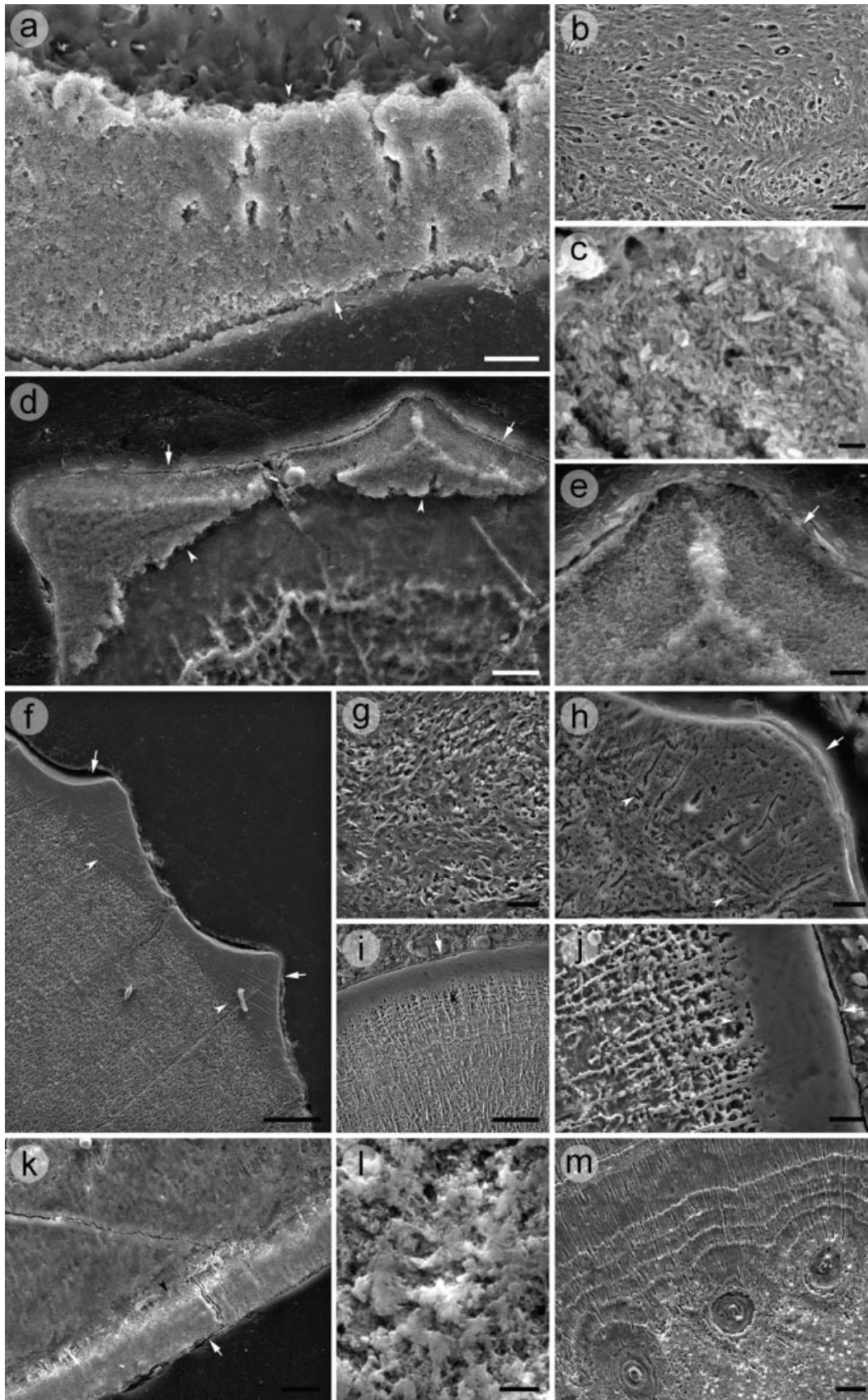


Figure 3

uted around the circumference of the tooth, with a thin layer covering the lingual and labial surfaces of the cusp, and a considerably thicker layer coating either side of the cusp (Fig. 4c). The transition from thin to thick covering is abrupt. Close examination of the capping tissue reveals abundant randomly arranged crystallites with a rounded or subrounded morphology (Fig. 4d). This contrasts with the highly porous and tubule-rich orthodentine that underlies that layer (Fig. 4e). The border between the two tissues is uneven, and dentine tubules extend up to, and probably across, the boundary (Fig. 4f). The position of this tissue around the circumference of the tooth, its hypermineralized nature and histological dissimilarity from dentine, and the probable presence of odontoblast cell processes within it are all indicative of SCE.

**Phoebodontiformes: *Jalodus australiensis*.**

The ridged tricuspid grasping teeth of *Jalodus australiensis* (BRSUG 27194) possess a superficial monolayer of undifferentiated SCE (Fig. 4g). A sharply defined enameloid–dentine junction is present, exemplified, in this case, by the differential etching properties of the enameloid monolayer and the underlying dentine, and microstructural features of the dentine core are not discernable. Enameloid appears to be present only on the labial surface of the cusp (though this may be an artifact of preparation, as the plane of section in Fig. 4g is slightly oblique). The enameloid is composed of randomly arranged rounded or subrounded hydroxyapatite crystallites (Fig. 4h), comparable in both size and morphology to those observed in the superficial hypermineralized capping tissue of *Orthacanthus* sp. (AMNH 7115).

**Symmoriiformes: *Akmonistion zangerli*.** The teeth of the stethacanthid *Akmonistion zangerli* (UMZC GN.1047) possess a thin monolayer of capping tissue that lacks microstructural differentiation (Fig. 4i). The cap tissue is easily distinguishable from the dentine core, and a relatively distinct junction is present between the two tissues, defined primarily by differential reactions of the two tissues to

etching, but also by differences in matrix quality. The dentine core is composed primarily of orthodentine, though a center of osteodentine comprising a series of small denteons is present. Dentine tubules traverse the junction and extend into the capping tissue (evident from the presence of numerous dentine tubule canals along the tissue boundary – Fig. 4j). The cap tissue, on the other hand, is hypermineralized, and individual hydroxyapatite crystallites of round or subround morphology are discernable (Fig. 4j). The presence of a uniform layer of the capping tissue around the circumference of the tooth, its hypermineralized nature, and the inclusion of odontoblast cell processes in the layer is indicative of (single crystallite) enameloid.

**Cladoselachiformes: *Cladoselache kepleri*.**

The teeth of *Cladoselache kepleri* (CMNH 5420) possess a poorly differentiated cap of hypermineralized tissue, organized into a thin monolayer with regular ridges (Fig. 4k). At certain points around the tooth, the layer is nearly impossible to detect (particularly in the area of thin covering between ridges). The hypermineralized cap tissue is composed of round or subround crystallites (Fig. 4l) resembling those in *Akmonistion zangerli*, *Jalodus australiensis*, and *Orthacanthus*, and while it differs histologically from the underlying dentine, a precise junction between the two tissues is, at times, difficult to identify (Fig. 4m). The dentine core is composed primarily of orthodentine. Dentine tubules can be seen extending into the cap and, in some instances, nearly reaching the outer enameloid surface (Fig. 4m). Once again, the presence of the tissue around the circumference of the tooth (and its organization into a series of regularly spaced ridges), the hypermineralized nature of the tissue, and its histological dissimilarity from dentine (and the prospective incorporation of odontoblast cell processes in the layer) is suggestive of SCE.

**Holocephali: *Helodus*.** The tooth plates of *Helodus* (BRSUG 27195) possess a well-differentiated hypermineralized cap of SCE (Fig. 5a). This enameloid

Fig. 3. Tooth microstructure of the non-neoselachians *Hybodus nebraskensis* (a–c), *Protacrodus serra* (d, e), *Ctenacanthus compressus* (f–h), *Ctenacanthus* sp. (i, j), and a Cleveland Shale “cladodont” shark (k–m). SEM (a) single crystallite enameloid monolayer of CM 44547, viewed in cross-section. Note the remnant spaces of odontoblast cell processes. Etched 5 s in 10% HCl. Scale bar = 5  $\mu$ m. (b) Cross-section through the orthodentine core of CM 44547. Etched 5 s in 10% HCl. Scale bar = 10  $\mu$ m. (c) Rod-shaped crystallites in the enameloid monolayer of CM 44547. Etched 5 s in 10% HCl. Scale bar = 1  $\mu$ m. (d) Cross-section through the ridged single crystallite enameloid monolayer of BRSUG 27193. Etched 5 s in 5% HCl. Scale bar = 12.5  $\mu$ m. (e) Rod-shaped enameloid crystallites of BRSUG 27193. Etched 5 s in 5% HCl. Scale bar = 4  $\mu$ m. (f) Overview of a cross-section through the ridged single crystallite enameloid monolayer of CMNH 9207. Etched 5 s in 5% HCl. Scale bar = 75  $\mu$ m. (g) Cross-section through the osteodentine core of CMNH 9207. Etched 5 s in 5% HCl. Scale bar = 20  $\mu$ m. (h) Detail of the single crystallite enameloid monolayer of CMNH 9207 in cross-section. Hypermineralization has obscured individual enameloid crystallites, but no microstructural differentiation is apparent within the layer. Etched 5 s in 5% HCl. Scale bar = 12.5  $\mu$ m. (i) The enameloid monolayer of CMNH 5290, in cross-section, shows no evidence of microstructural differentiation. Etched 5 s in 5% HCl. Scale bar = 50  $\mu$ m. (j) Individual enameloid crystallites are not discernable in CMNH 5290, but numerous odontoblast cell processes appear to extend across the enameloid–dentine junction. Etched 5 s in 5% HCl. Scale bar = 15  $\mu$ m. (k) A distinct single crystallite enameloid monolayer is discernable in a cross-section through CMNH 5121. Etched 5 s in 5% HCl. Scale bar = 120  $\mu$ m. (l) Randomly oriented crystallites that comprise the enameloid monolayer of CMNH 5121. Etched 5 s in 5% HCl. Scale bar = 2.5  $\mu$ m. (m) A cross-section through the dentine core of CMNH 5121 reveals a center of osteodentine with numerous denteons, surrounded by concentrically deposited pallial orthodentine. Etched 5 s in 5% HCl. Scale bar = 30  $\mu$ m. Arrowheads denote the enameloid–dentine junction.

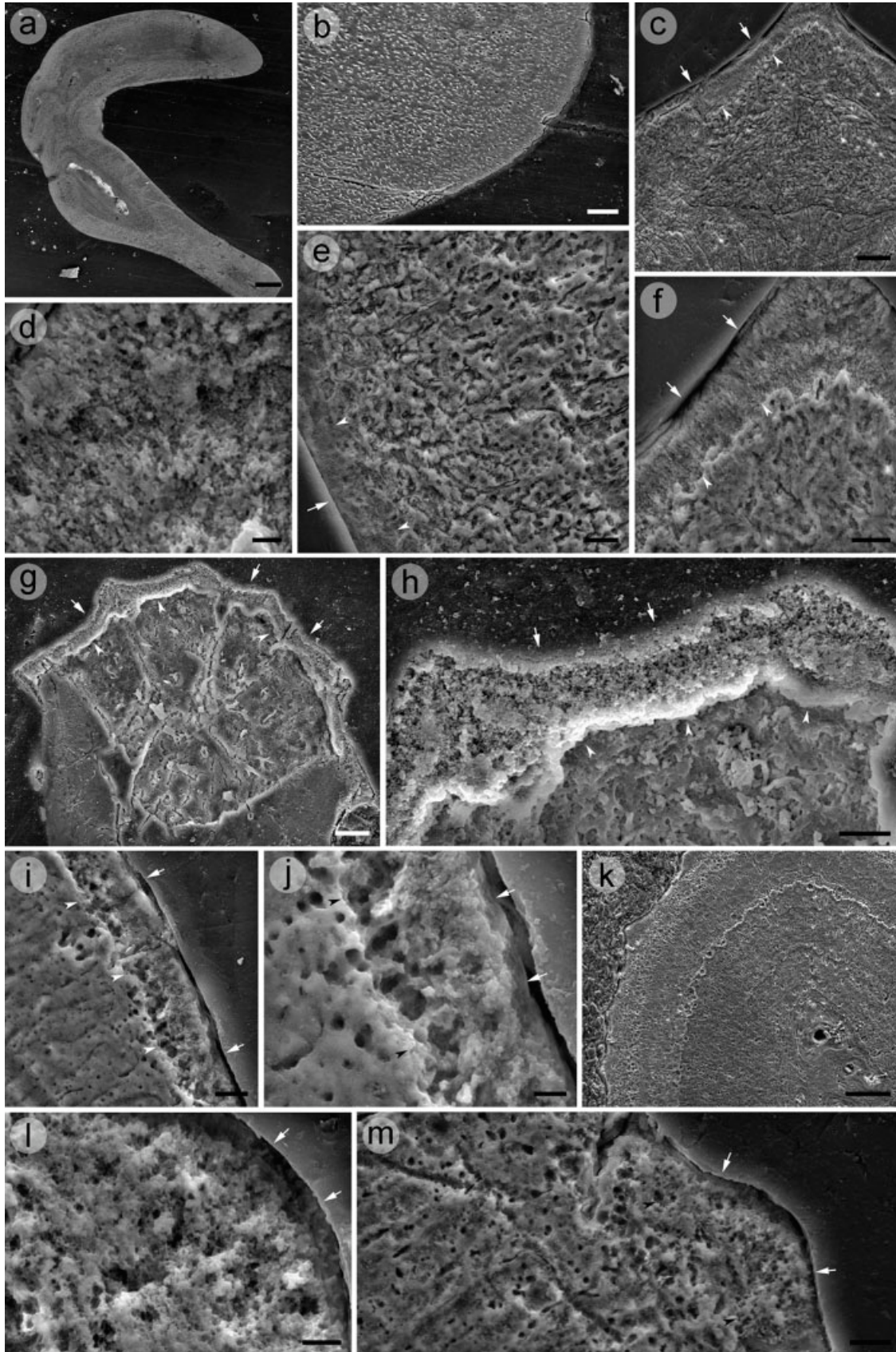


Figure 4

loid monolayer coats the oral surface of the plate, as well as the inner face of the plate's numerous surface pores, and is easily distinguished from the dentine core of the tooth. A sharp enameloid–dentine junction exists between the enameloid and the dentine core, and traces of odontoblast cell processes can be seen extending through the hypermineralized surface layer, nearly reaching the surface of the tooth plate (Fig. 5b). In terms of crystallite morphology, the enameloid is composed of small round to subround hydroxyapatite crystallites (Fig. 5c), resembling those making up the SCE of *Cladoselache kepleri*, *Akmonistion zangerli*, *Jalodus australiensis*, and *Orthacanthus*.

## DISCUSSION

Our systematic assessment of chondrichthyan tooth microstructure reveals that non-neoselachian chondrichthyans (i.e., *Cladoselache kepleri*, *Akmonistion zangerli*, *Orthacanthus* sp., *Jalodus australiensis*, *Ctenacanthus compressus*, *Ctenacanthus* sp., “cladodonts,” *Protacrodus serra*, and *Hybodus nebraskensis*), as well as a basal holocephalan (*Helodus*, Lund and Grogan, 1997), possess a monolayer of hypermineralized capping tissue resembling SCE. The tissue capping the teeth of these taxa is interpreted here as enameloid based on its position in the tooth (superficial, generally covering the entire crown), its appearance, and composition (hypermineralized, composed of discernable crystallites; reacts differentially to etching than underlying dentine, often accentuating a distinct enameloid–dentine junction; contains traces of odontoblast tubules) and its microstructure (composed of randomly oriented single crystallites, and lacking lines of incremental growth). An analysis of the distribution of enameloid within Chondrichthyes (in the context of alternative hypotheses of chondrichthyan intrarelationships – Fig. 6) provides strong phylogenetic evidence for the presence of a SCE monolayer

in the primitive chondrichthyan tooth, and the acquisition of a triple-layered enameloid fabric (SLE composed of single crystallites, as well as PFE and TFE) along the neoselachian stem.

Comparative studies of character evolution must be carried out within the bounds of a phylogenetic framework. Only after plotting character states on a phylogeny can we classify conditions as “primitive” or “derived,” and elucidate the polarity of morphological (or molecular) change (Smith, 1994; Raff, 1996). In the case of chondrichthyans, there are several published phylogenetic hypotheses that differ considerably with respect to tree topology (Schaeffer and Williams, 1977; Young, 1982; Maisey, 1984, 2001; Gaudin, 1991; Coates and Sequeira, 2001a,b; Ginter, 2005), and attempts to generate a single consensus phylogeny by employing supertree methodology (Bininda-Emonds et al., 2002) failed (data not shown). As a result of the rampant and irreconcilable incongruence among these phylogenies, we have analyzed our paleohistological data separately, in light of each of the aforementioned phylogenetic hypotheses. Note that the conclusions discussed below are broadly supported by all of these phylogenies, and are not contingent upon tree selection.

According to the phylogenies of Schaeffer and Williams (1977), Young (1982), and Gaudin (1991) (Fig. 6a,b,d), holocephalans lie at the base of the Chondrichthyes, as the sister taxon to all other chondrichthyans (i.e. the “sharks”). The presence of SCE on the tooth plates of *helodus*, a basal stem holocephalan (Lund and Grogan, 1997), therefore provides support for the presence of enameloid on the primitive chondrichthyan tooth. Enameloid is also present in a number of successively crownward taxa in these phylogenies, including the symmoriiform *Akmonistion*, *Cladoselache*, *Ctenacanthus*, the xenacanthiform *Orthacanthus*, and the hybodontiform *Hybodus*. *Cladoselache* falls at the base of the chondrichthyan tree in the phylogeny of Maisey (1984) (Fig. 6c), again supporting the presence of

Fig. 4. Tooth microstructure of the non-neoselachians *Orthacanthus compressus* (a, b), *Orthacanthus* sp. (c–f), *Jalodus australiensis* (g, h), *Akmonistion zangerli* (i, j), and *Cladoselache kepleri* (k–m). SEM (a) A longitudinal section through CM 44556. Etched 5 s in 5% HCl. Scale bar = 250  $\mu$ m. (b) The surface of CM 44556, viewed in longitudinal section, lacks an enameloid cap. Etched 5 s in 5% HCl. Scale bar = 2  $\mu$ m. (c) A cross-section through AMNH 7115. Etched 5 s in 5% HCl. Scale bar = 30  $\mu$ m. (d) Detail of the single crystallite enameloid of AMNH 7115 in cross-section. The layer lacks microstructural differentiation, and is composed of round to subround crystallites. Etched 5 s in 5% HCl. Scale bar = 3  $\mu$ m. (e) Remnants of odontoblast cell processes in a cross-section through the dentine core of AMNH 7115. Etched 5 s in 5% HCl. Scale bar = 12.5  $\mu$ m. (f) In cross-section, the border between enameloid and dentine in AMNH 7115 is uneven, but distinct. Dentine pores are present along the enameloid–dentine junction. Etched 5 s in 5% HCl. Scale bar = 10  $\mu$ m. (g) A cross-section through BRSUG 27194 reveals a well-defined monolayer of single crystallite enameloid on the labial surface of the tooth cusp. Etched 5 s in 10% HCl. Scale bar = 15  $\mu$ m. (h) The enameloid monolayer of BRSUG 27194 exhibits no microstructural differentiation, and is composed of round or subround crystallites. Etched 5 s in 10% HCl. Scale bar = 5  $\mu$ m. (i) A cross-section through UMZC GN.1047 reveals a thin monolayer of single crystallite enameloid overlying orthodentine. Etched 5 s in 5% HCl. Scale bar = 7.5  $\mu$ m. (j) The enameloid monolayer of UMZC GN.1047 shows no microstructural differentiation, and is composed of round to subround crystallites. Etched 5 s in 5% HCl. Scale bar = 2.5  $\mu$ m. (k) The tooth cusp of CMNH 5420, viewed in cross-section, is composed of a primarily orthodontinuous core, capped by a ridged monolayer of single crystallite enameloid. Etched 5 s in 10% HCl. Scale bar = 60  $\mu$ m. (l) The monolayer of single crystallite enameloid in CMNH 5420 is composed of round or subround crystallites. Etched 5 s in 10% HCl. Scale bar = 4  $\mu$ m. (m) A precise border between the single crystallite enameloid monolayer and the underlying orthodentine is difficult to discern in CMNH 5420. The presence of numerous dentine pores along the tissue boundary suggests that odontoblast cell processes extended into the enameloid cap. Etched 5 s in 10% HCl. Scale bar = 7.5  $\mu$ m. Arrows denote the outer enameloid surface. Arrowheads denote the enameloid–dentine junction.

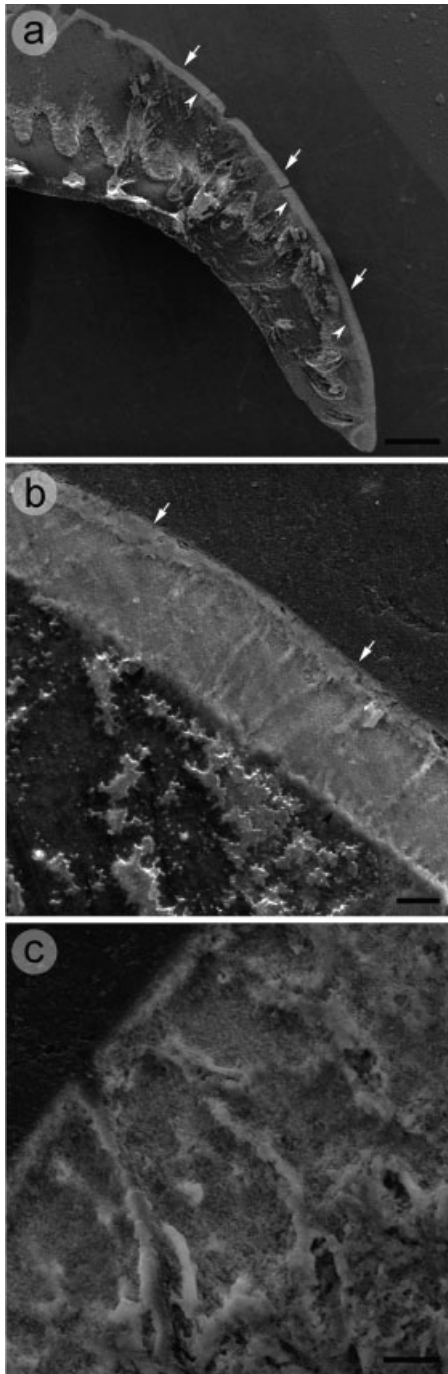


Fig. 5. Tooth plate microstructure of the basal holocephalan *Helodus*. SEM (a) A longitudinal section through the tooth plate of BRSUG 27195. The dentinous base of the plate is capped by a hypermineralized monolayer of single crystallite enameloid. Etched 10 s in 5% HCl. Scale bar = 250  $\mu\text{m}$ . (b) The surface of BRSUG 27195, viewed in longitudinal section, is covered with a monolayer of enameloid lacking microstructural differentiation. A well-defined enameloid–dentine junction is present. Etched 10 s in 5% HCl. Scale bar = 12.5  $\mu\text{m}$ . (c) The single crystallite enameloid of BRSUG 27195 is composed of round or subround crystallites. Etched 5 s in 10% HCl. Scale bar = 10  $\mu\text{m}$ . Arrows denote the outer enameloid surface. Arrowheads denote the enameloid–dentine junction.

enameloid in the ancestral chondrichthyan tooth. Coates and Sequeira (2001a,b) divide chondrichthyans into two clades: one comprising *Cladoseleche*, the Symmoriiformes and the holocephalans (with *Cladoseleche* and the Symmoriiformes as stem holocephalans) and one comprising the Xenacanthiformes, Ctenacanthiformes and Hybodontiformes. While the teeth of *Denaea* and *Cobelodus* (the most basal taxa in the *Cladoseleche*/symmoriiform/holocephalan clade) were not sampled in this study, we demonstrate the widespread presence of enameloid on the teeth taxa in both clades (including many basal taxa – Fig. 6f). Finally, teeth of the most basal chondrichthyan taxa in the phylogenies of Maisey (2001) (Fig. 6e) and Ginter (2005) (Fig. 6g), *Pucapampella* and *Antarctilamna*, respectively, were not sampled, though once again, enameloid was present on the teeth of successively crownward basal chondrichthyans in both of these trees. The widespread basal distribution of tooth enameloid in these seven phylogenies provides strong support for the presence of a SCE cap on the ancestral chondrichthyan tooth. The implications of this are discussed below.

#### Enameloid Microstructure as a Preadaptation to Crown Group Neoselachian Tooth Function

The radiation of the crown group Neoselachii during the Jurassic and Cretaceous has been attributed, in large part, to the evolution of complex hunting and feeding strategies in response to an increase in prey (i.e., actinopterygian) abundance and diversity (Thies and Reif, 1985). These strategies rely upon a number of derived anatomical features, including a segmented and calcified notochordal sheath with calcified cartilage vertebrae for faster swimming, modification of pelvic and pectoral fins and their articulation for greater maneuverability, and modifications of the jaw suspensorium (Moss, 1972, 1977; Maisey, 1980, 1986). Furthermore, many neoselachians also possess sharp cutting and gouging teeth that are shed rapidly and replaced continuously throughout life (Moss, 1967; Luer et al., 1990). This is in contrast to the multicuspoid clutching and grasping teeth of most stem neoselachians which, in the case of some cladodont sharks, were retained beneath the skin of the outer jaw margin, rather than shed, following replacement (Williams, 1990, 2001).

Sharks in the neoselachian crown group often employ predatory techniques such as biting in conjunction with lateral headshakes to gouge flesh from prey, placing the teeth under tremendous bending stress. Functional morphological studies by Preuschoft et al. (1974) have demonstrated that the PFE of neoselachian teeth effectively prevents crack propagation and imparts tensile strength, while TFE beneath the PFE imparts considerable resistance to compressive force.

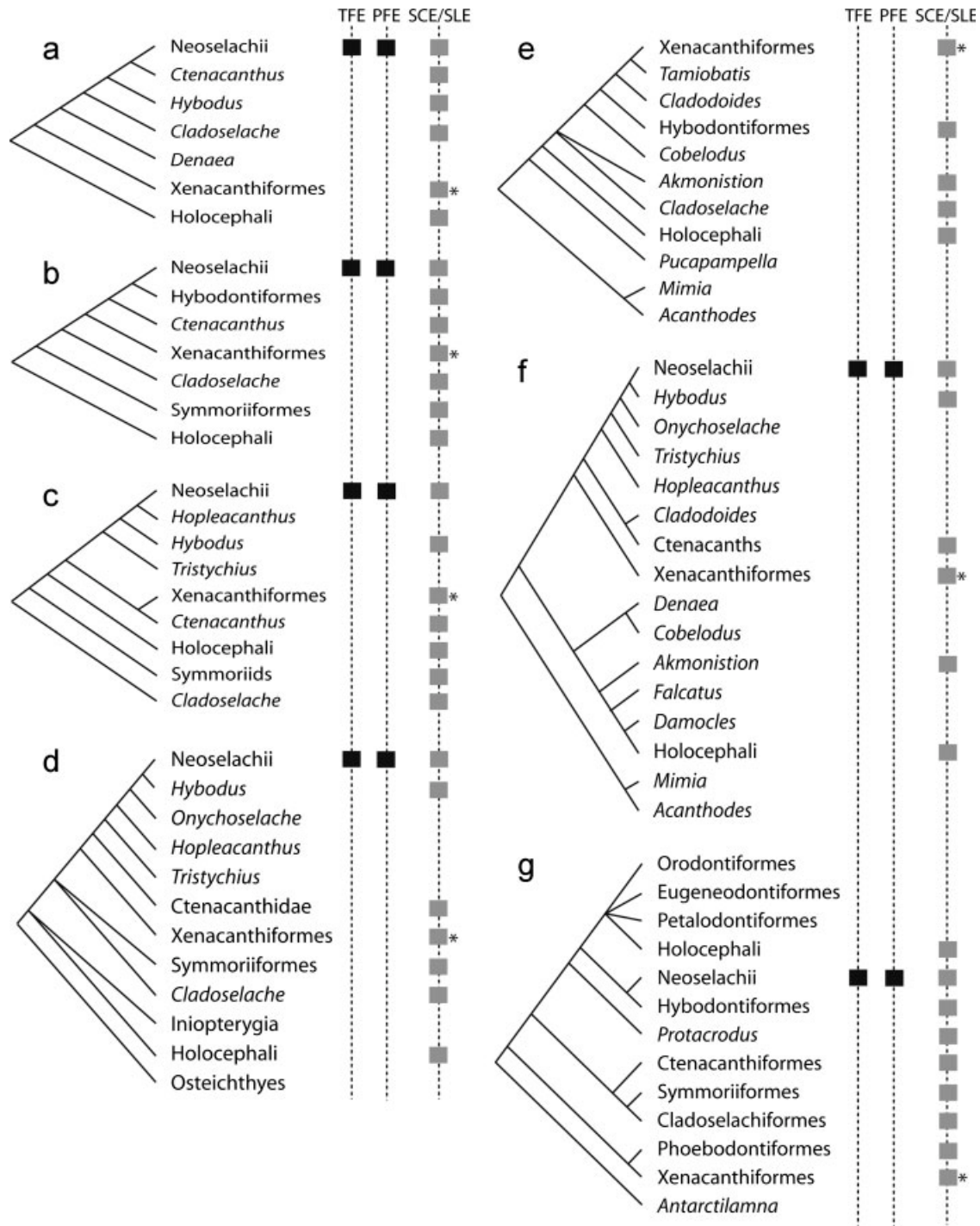


Fig. 6. Chondrichthyan phylogenies by (a) Schaeffer and William (1977), (b) Young (1982), (c) Maisey (1984), (d) Gaudin (1991), (e) Maisey (2001), (f) Coates and Sequeira (2001a,b), and (g) Ginter (2005), with the distribution of tooth enameloid microstructure on each. Asterisk (\*) indicates that only one of two sample xenacanthiform taxa sampled possessed SCE. SCE/SLE, single crystalline enameloid/shiny layer enameloid; PFE, parallel-fibered enameloid; TFE, tangle-fibered enameloid.

It therefore appears that enameloid microstructure plays a considerable role in the maintenance of neoselachian tooth integrity during feeding.

The neoselachian crown group can be subdivided into two clades (Fig. 7): the Galea (roughly synony-

mous with the galeomorphs of Compagno, 1973) and the Squalea (includes orbitostylic sharks, skates and rays; Shirai, 1996). Cladistic analysis of morphological data from extant crown neoselachians place *Heterodontus* as the basal most galean, and *Chlamydosela-*

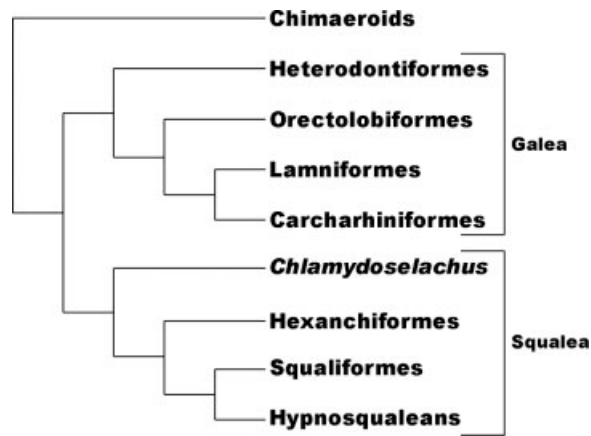


Fig. 7. Phylogenetic interrelationships of the crown group Neoselachii. Based on the cladistic analysis of morphological data by Shirai (1996), with some clades collapsed for simplicity.

*chus* as the basal most squalian (Shirai, 1992, 1996). *Heterodontus* possesses a unique dentition, with clutching and grasping teeth in the anterior region of the jaw, and flattened crushing teeth at the back (Summers et al., 2004). A histological examination of the teeth of *Heterodontus* revealed that the front teeth possess a fully differentiated triple-layered enameloid fabric (a shiny layer of SCE, PFE, and TFE), while the back teeth possess layer of TFE underlying a thick layer of SCE (Reif, 1977; Cuny et al., 2000). Reif (1977) proposed that the reduction of the enameloid layer in the back teeth of *Heterodontus* was an adaptation to durophagy.

The teeth of *Chlamydoselachus* are fine, recurved, and tricuspid, and are striking analogues of the clutching and grasping teeth of the non-neoselachian Phoeodontiformes (Ginter and Ivanov, 1996; Ginter, 2000; Ginter et al., 2002). Furthermore, *Chlamydoselachus* lacks the enlarged rostrum and ventral mouth of more derived neoselachians, and instead possesses a jaw articulation that lies in level with the otic region of the skull, a feature shared with non-neoselachian elasmobranchs (Shaeffer, 1967; Zangerl, 1973). It is therefore likely that the predatory strategies employed by *Chlamydoselachus* are analogous to those employed by Palaeozoic sharks (i.e., clutching and grasping predation), and quite unlike the cutting and gouging strategies employed by more derived forms.

We demonstrate that the teeth of *Chlamydoselachus anguineus* possess a fully differentiated triple-layered enameloid microstructure, and the confirmed presence of this dental feature in the basal-most members of both crown neoselachian clades implies its presence in the last common ancestor of all crown group neoselachians. However, given the predatory tactics employed by these taxa (clutching and grasping in *Chlamydoselachus*, and durophagy in *Heterodontus*) it is highly unlikely that this

ancestor possessed teeth that functioned in cutting and gouging predation. It therefore appears that the triple-layered enameloid microstructure phylogenetically predates the advent of cutting and gouging teeth, and is thus a case of preadaptation or "exaptation" (Gould and Vrba, 1982).

Recent analyses (Maisey et al., 2004) suggest, contrary to Shirai 1992, 1996, that the batoids (skates and rays) are not derived squalians, but rather the sister group to all other neoselachians (i.e. the sister group to the Galea and Squalea). Such a phylogenetic placement of the batoids disagrees with the view that the most primitive neoselachian teeth possessed triple-layered enameloid (as the batoid dentition is reported to possess a single layer of TFE). However, it does not conflict with our argument that a triple-layered enameloid fabric was a preadaptation to the neoselachian cutting and gouging tooth function (as batoids are durophagous).

Cuny et al. (2001) report the presence of two-layered enameloid—an outer layer of compact SCE, and an inner layer SCE, though with some crystallites organized into parallel bundles lying perpendicular to the enameloid–dentine junction—in the Hybodontiformes *Acrodus* and *Polyacrodus*, and this may represent a precursor to the neoselachian triple-layered fabric. The teeth of these Hybodontiformes are rather flat and low-crowned, and were not likely subject to excessive bending forces, and it is therefore highly unlikely that the fiber bundles lying perpendicular to the enameloid–dentine junction of these teeth was adaptive. Rather, the appearance of these microstructures may best be explained as the fortuitous consequence of modification to the odontogenetic developmental program which, when combined with additional modifications of the jaws and axial skeleton, facilitated the evolution of novel and complex predatory strategies.

### The Relationship Between Enamel, Chondrichthyan Enameloid, and Actinopterygian Enameloid

Enamel and enameloid are hypermineralized cap tissues that differ considerably in terms of both microstructure and organic matrix composition, and these differences have been attributed to a heterochronic shift in ameloblast differentiation during odontogenesis (Smith and Hall, 1993; Smith, 1995). Enamel is a monotypic tissue, and forms through the outer apposition of successive layers of proteinaceous ameloblastic cell secretions (primarily amelogenin) following the mineralization of the underlying dentine matrix (Smith, 1995; Satchell et al., 2002). Consequently, enamel exhibits incremental lines of growth, and the junction between dentine and enamel corresponds to the basal lamina of the inner dental epithelium (Smith, 1995). Conversely, enameloid is the bitypic product of mixed ameloblastic and odontoblastic cell secretions, and results

from the differentiation of ameloblasts prior to the mineralization of underlying dentine (Smith, 1992). Enameloid matrix contains collagen of ectomesenchymal origin and odontoblast cell processes, in addition to ameloblastic cell secretions (primarily enamelin, though amelogenin and other enamel proteins are also present [Herold et al., 1980; Satchell et al., 2002]), and is secreted beneath the basal lamina of the inner dental epithelium (Shellis and Miles, 1974, 1976; Shellis, 1975; Kemp, 1985; Smith, 1995). There is evidence that the shift from enamel to enameloid has occurred on several occasions during vertebrate evolution (Donoghue et al., 2000; Donoghue, 2001).

During enamel biomineralization, ameloblast-derived matrix proteins aggregate to form compartments within which hydroxyapatite crystallites are precipitated (Diekwisch et al., 1993, 1995). The biomineralization of enameloid differs considerably from that of enamel, and also exhibits variation among gnathostome lineages (i.e., between chondrichthyans and actinopterygians). In chondrichthyans, enameloid crystallites precipitate almost exclusively upon odontoblast-derived tubular vesicles, delimited by a unit membrane, and although collagen and other “electron-dense fibrils” are present in the matrix, they do not serve as a crystallite nucleation structures (Prostak and Skobe, 1988; Sasagawa, 1989). In contrast, actinopterygian enameloid crystallites precipitate initially upon matrix vesicles, and accumulate subsequently along collagen fibers (Sasagawa, 1997). Furthermore, the mineralization of actinopterygian enameloid commences at the enameloid–dentine junction and progresses toward the outer enameloid surface, while mineralization of elasmobranch enameloid generally occurs throughout the layer, with no discrete front (Sasagawa, 2002 – though see Fossé et al., 1974; Risnes, 1990; Cuny and Risnes, 2005). These differences in matrix composition and mineralization patterns have led many to regard elasmobranch enameloid (“coronoïn” [Bendix-Almgreen, 1983]) and actinopterygian enameloid (“acrodin” [Ørving, 1978]) as two distinct products of convergent evolution, despite previous assertions of homology (Moss, 1977). In addition, the alleged absence of enameloid on the teeth and fin spines of *Cladoseleache* (initially noted by Dean, 1909), and its reported absence from the teeth and dermal denticles of other basal elasmobranchs (Ørving, 1966; Gross, 1973) provides evidence (albeit patchy and often anecdotal) for the acquisition of enameloid as a synapomorphy of “higher” elasmobranchs. There are reports of superficial enameloid-like tissue capping the tooth plates of chimaerid holocephalans (Ørving, 1985). However, the phylogenetic position of holocephalans within the Chondrichthyes has long been a matter of much contention among systematists, and this has precluded their use as an indicator of the plesiomorphic chondrichthyan dental condition.

We note the presence of a SCE monolayer on the tooth plates of the basal holocephalan *Helodus*, as well as on the teeth of several non-neoselachian chondrichthyans (Fig. 6). The phylogenetic distribution of this tissue highlights tooth enameloid as a probable chondrichthyan plesiomorphy. Enameloid (or “durodentine,” a term synonymous with “mesodermal enamel,” or enameloid) has been observed in the developing teeth of the basal neopterygian *Polypterus* (Meinke, 1982), as well as in the fossil teeth of *Andreolepis hedei*, the most primitive known teleostome fish (Janvier, 1978). The presence of enameloid in basal holocephalan tooth plates, as well as the ubiquitous presence of enameloid in the teeth of actinopterygians (and most notably, at the base of the Teleostomi), implies its presence in the teeth of the last common ancestor of the gnathostome crown group. We, therefore, argue that the tooth enameloid of chondrichthyans and actinopterygians are, in fact, homologous tissues, and that the observed differences between enameloid matrix composition and mineralization in the two groups are the result of lineage-specific divergence from the primitive state.

#### A Developmental Model of Chondrichthyan Enameloid Evolution

In the enameloid of crown neoselachians, crystallites are arranged into discrete bundles of varying orientation, and this differs considerably from the SCE of holocephalans and stem group neoselachians. Reif (1979) postulated that the organic matrix of the thin layer of SCE overlying the PFE of neoselachian teeth is derived almost exclusively from ameloblastic cell products, due to its position at the outer enameloid surface and probable formation in complete isolation from odontoblast cell secretions. While there is still much debate regarding the specific control of enameloid crystallite orientation and the development of “higher order structures” (i.e., crystallite bundles) within the layer, it is broadly accepted that odontoblast-derived cell products (namely, tubular vesicles) play a fundamental role in the initiation and direction of crystallite growth (Prostak et al., 1990; Sasagawa, 2002). If a mixed matrix composed of both ameloblast cell secretions and odontoblast-derived tubular vesicles is, in fact, critical to the development of higher order enameloid structures, then a deficiency of such vesicles (i.e., their presence below a “threshold quantity”) may inhibit the development of enameloid that is microstructurally more complex than a monolayer of randomly oriented single crystallites. Conceivably, a heterochronic shift in ameloblast differentiation (Fig. 8) during odontogenesis (from “late” differentiation, near the end of dentinogenesis, in stem neoselachians, to an “early” differentiation in crown neoselachians), comparable to the mechanism underlying the evolution of enamel from

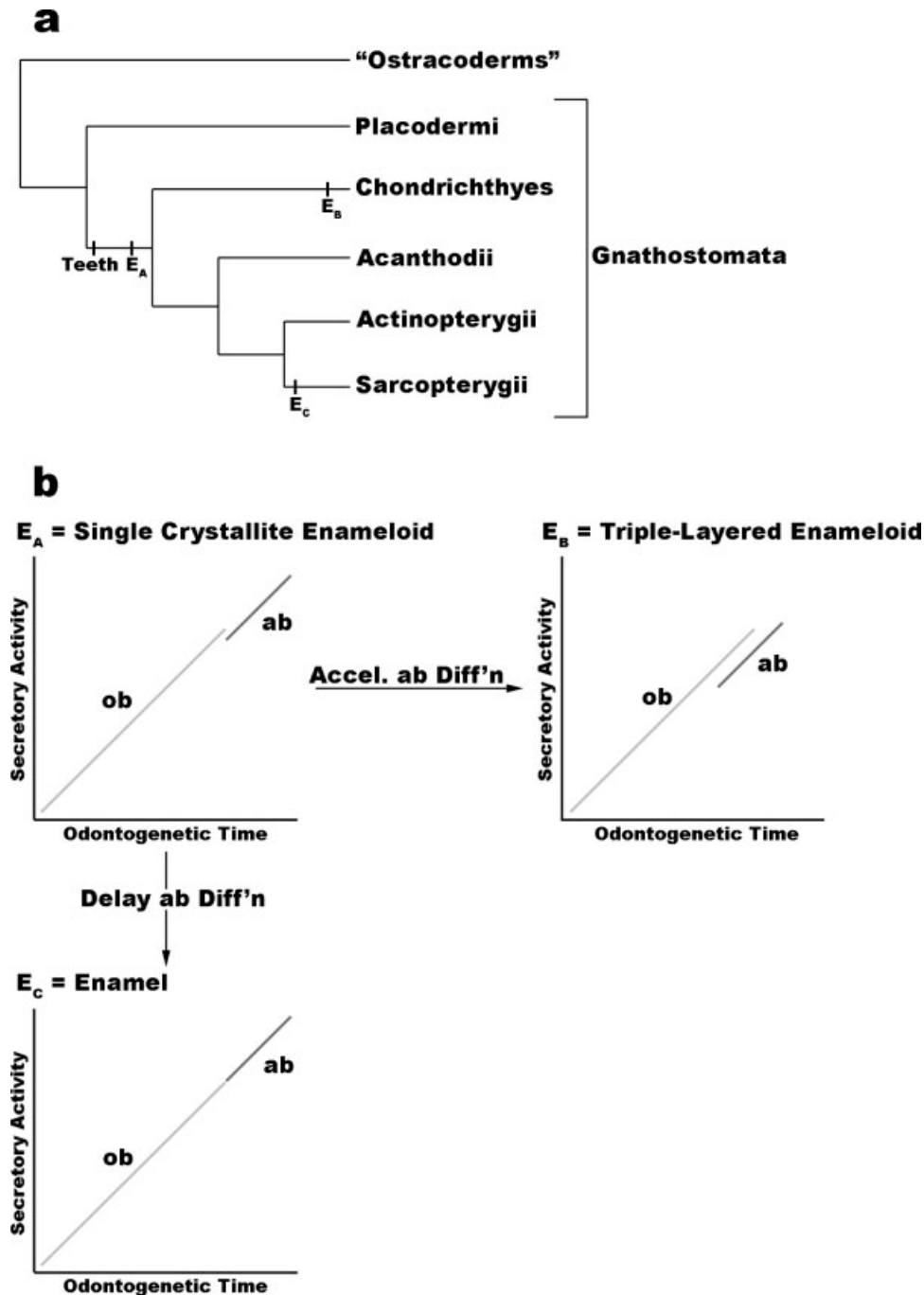


Fig. 8. Gnathostome phylogeny, and a heterochrony-based explanation of the evolution of hypermineralized dental cap tissues in toothed vertebrates. (a) Interrelationships of the major gnathostome groups (based on Donoghue and Sansom, 2002). The origin of teeth and known hypermineralized dental cap tissue conditions are indicated. (b) The plesiomorphic gnathostome condition is a tooth with a superficial capping layer of single crystallite enameloid ( $E_A$ ), resulting from a late differentiation of ameloblasts during odontogenesis (an enameloid matrix that is rich in ameloblastic cell secretions, and deficient in odontoblast cell products). A heterochronic shift to earlier ameloblast differentiation along the chondrichthyan lineage produces an enameloid matrix that is richer in odontoblast cell products (namely, tubular vesicles), and is thus able to support microstructural differentiation through the development of crystallite bundles, resulting in the neoselachian triple-layered enameloid fabric ( $E_B$ ). Such a mechanism (though in reverse, with delayed differentiation of ameloblasts, and deposition of ameloblast cell secretions upon mineralized dentine) underlies the evolution of sarcopterygian enamel ( $E_C$ ) from enameloid (Smith, 1995): ab, ameloblast; ob, odontoblast.

enameloid across vertebrate phylogeny (Smith, 1995), could permit a greater incorporation of odontoblast-derived tubular vesicles into the enameloid

matrix. This, in turn, could result in the generation of suitable matrix support for the growth of higher order enameloid microstructures.

### The Presence of Enameloid in the Primitive Gnathostome Tooth

Implicit in the hypothesis of chondrichthyan and actinopterygian enameloid homology is the homology of gnathostome teeth themselves. Conventionally, it is argued that teeth originated once, in (or along the stem leading to) the last common ancestor of chondrichthyans and osteichthyans, from dermal denticles located along the margin of the mouth (Reif, 1982). Conversely, Smith (2003) and Smith and Johanson (2003) suggest that teeth may have originated independently at least twice (in placoderms and all other gnathostomes), and possibly up to four times (in placoderms, chondrichthyans, acanthodians and osteichthyans). This hypothesis is based on two lines of evidence: 1) The presence of "true teeth" on the gnathals of arthrodire placoderms, and the supposed absence of teeth in basal chondrichthyans, acanthodians, and osteichthyans (Johanson and Smith, 2003; Smith and Johanson, 2003) and 2) inferred differences in dentition patterning among the four major gnathostome lineages (Smith, 2003).

Recently described dental elements on the supragnathals and infragnathals of arthrodire placoderms are classified as "true teeth" by Smith and Johanson (2003) based on their apparent occurrence in patterned and regulated rows, and their histological composition of tubular dentine. Presumably derived from pharyngeal denticles (Johanson and Smith, 2003), these "teeth" lack an enameloid cap. However, the classification of such arthrodire denticles as "true teeth" is contentious. Arthrodire oral denticles closely resemble tubercles or denticles of the dermal skeleton in other early vertebrates (Burrow, 2003), and a regular pattern of addition (similar to that observed in teeth, though arrived at independently) has been proposed for placoderm (dermal) marginal plate denticles (Young, 1986). Furthermore, tubular dentine is not restricted to "true teeth," as is demonstrated by its presence in the marginal spine plate denticles of the placoderm dermal skeleton, as well as in elements of the dermal skeletons of various other jawless and jawed vertebrates (Burrow, 2003). Evidence for the absence of teeth in basal chondrichthyans and osteichthyans is equally circumstantial, and is limited to the apparent absence of teeth from early chondrichthyan and osteichthyan microvertebrate remains (Sansom et al., 1996; Williams, 2001; Smith and Johanson, 2003). Finally, while there are toothless acanthodians, some phylogenies place toothed forms (namely, ischnacanthiforms and climatiforms) at the base of the Acanthodii (Long, 1986; Janvier, 1996). It should be noted, however, that nearly all acanthodian phylogenies are weakly supported, and that acanthodian monophyly itself is currently a matter of much contention among early vertebrate paleontologists.

Smith (2003) cites differences in dentition patterning in the four major gnathostome lineages as additional evidence for the independent origin of teeth. Assuming that teeth are not derived from dermal denticles, but rather, from pharyngeal denticle sets, it is suggested that such denticles may have been co-opted as teeth and patterned independently in different fish groups. There is, however, no published molecular evidence in support of either a pharyngeal (i.e., endodermally-induced rather than ectodermally-induced) origin of teeth, nor for the dentition patterning differences proposed by Smith (2003). We thus maintain that "true" teeth originated once in Gnathostomata, along the stem leading to the last common ancestor of chondrichthyans and osteichthyans (Fig. 8, a dermal or pharyngeal origin of true teeth is equivocal). Furthermore, using the basal chondrichthyan condition as a proxy for that of the last common ancestor of crown gnathostomes, we hypothesize that this ancestral gnathostome tooth possessed a hypermineralized cap of SCE.

### CONCLUSIONS

All non-neoselachian sharks (with the exception of some Xenacanthiformes) and basal holocephalans appear to possess hypermineralized dental cap tissue that can be classified as enameloid. Plesiomorphically, chondrichthyan teeth possessed a superficial monolayer of SCE, providing phylogenetic support for the presence of SCE in the primitive gnathostome tooth, as well as the homology of elasmobranch and actinopterygian enameloid. Furthermore, the evolution of dental cap tissues in chondrichthyans and the appearance of a complex triple-layered enameloid fabric in neoselachians may have been modulated by the same heterochronic mechanism that underlies shifts between enamel and enameloid across vertebrate phylogeny. Finally, the occurrence of fully-differentiated neoselachian enameloid microstructure in the basal squalan *Chlamydoselachus anguineus*, and reports of the same in the basal galean *Heterodontus*, is evidence that triple-layered enameloid microstructure was a preadaptation to the cutting and gouging function of many neoselachian teeth, and may have played an integral role in the Mesozoic radiation of crown Neoselachii.

### ACKNOWLEDGMENTS

We thank Mike Coates (University of Chicago), Jennifer Clack (Cambridge University), John Maisey, Ivy Rutzky and Barbara Brown (American Museum of Natural History), Gary Jackson and Michael Ryan (Cleveland Museum of Natural History), Michał Ginter (University of Warsaw) and Liz Downey (London Aquarium) for facilitating access to the material upon which this study was based. Thanks also to Stuart Kearns and Remmert

Schouten (University of Bristol) for valuable technical assistance. No stem group neoselachians were harmed in the making of this paper.

## LITERATURE CITED

- Bendix-Almgreen SE. 1983. Carcharodon megalodon from the upper Miocene of Denmark, with comments on elasmobranch tooth enameloid: Coronoin. Bull Geol Soc Denmark 32:1–4.
- Bininda-Emonds ORP, Gittleman JL, Steel MA. 2002. The (super) tree of life: Procedures, problems, and prospects. Annu Rev Ecol Syst 33:265–289.
- Burrow CJ. 2003. Comment on “separate evolutionary origins of teeth from evidence in fossil jawed vertebrates.” Science 300:1661.
- Cappetta H, Duffin CJ, Zidek J. 1993. Chondrichthyes. In: Benton MJ, editor. The Fossil Record 2. London: Chapman and Hall. pp 593–609.
- Coates MI, Sequeira SEK. 2001a. A new Stethacanthid chondrichthyan from the Lower Carboniferous of Bearsden, Scotland. J Vert Pal 21:438–459.
- Coates MI, Sequeira SEK. 2001b. Early sharks and primitive gnathostome interrelationships. In: Ahlberg PE, editor. Major Events in Early Vertebrate Evolution: Palaeontology, Phylogeny, Genetics and Development. London: Taylor & Francis. pp 241–262.
- Compagno LJV. 1973. Interrelationships of living elasmobranchs. Zool J Linn Soc 53 (Suppl 1):15–61.
- Cuny G, Risnes S. 2005. The enameloid microstructure of the teeth of synechodontiform sharks (Chondrichthyes: *Neoselachii*). Pal Arch 3:8–19.
- Cuny G, Martin M, Rauscher R, Mazin J-M. 1998. A new neoselachian shark from the Upper Triassic of Grozon (Jura, France). Geol Mag 135:657–668.
- Cuny G, Hunt A, Mazin J-M, Rauscher R. 2000. Teeth of enigmatic neoselachian sharks and an ornithischian dinosaur from the uppermost Triassic of Lons-le-Saunier (Jura, France). Palaeont Z 74:171–185.
- Cuny G, Rieppel O, Sander PM. 2001. The shark fauna from the Middle Triassic (Anisian) of North-Western Nevada. Zool J Linn Soc 133:285–301.
- Dean B. 1909. Studies on fossil fishes (sharks, chimaeroids and arthroires). Mem Am Mus Nat Hist 9:211–287.
- Diekwisch T, David S, Bringas P Jr, Santos V, Slavkin HC. 1993. Antisense inhibition of AMEL translation demonstrates supra-molecular controls for enamel HAP crystal growth during embryonic mouse molar development. Development 117:471–482.
- Diekwisch TG, Berman BJ, Gentner S, Slavkin HC. 1995. Initial enamel crystals are not spatially associated with mineralized dentine. Cell Tissue Res 279:149–167.
- Donoghue PCJ. 2001. Microstructural variation in conodont enamel is a functional adaptation. Proc R Soc Lond B 268:1691–1698.
- Donoghue PCJ, Sansom IJ. 2002. Origin and evolution of vertebrate skeletonization. Microsc Res Technol 59:352–372.
- Donoghue PCJ, Forey PL, Aldridge RJ. 2000. Conodont affinity and chordate phylogeny. Biol Rev 75:191–251.
- Duffin C. 1980. A new euselachian shark from the upper Triassic of Germany. N Jb Geol Paläont Mh 1:1–16.
- Fossé G, Risnes R, Holmbakken N. 1974. Mineral distribution and mineralization pattern in the enameloid of certain elasmobranchs. Arch Oral Biol 19:771–780.
- Gaudin TJ. 1991. A re-examination of elasmobranch monophyly and chondrichthyan phylogeny. N Jb Geol Paläont Abh 182: 133–160.
- Ginter M. 2000. Late Famennian pelagic shark assemblages. Acta Geol Pol 50:369–386.
- Ginter M. 2005. The euselachian type of tooth-bases in Palaeozoic chondrichthyans. In: Hairapetian V, Ginter M, editors. Devonian Vertebrates of the Continental Margins. pp 11–12. Ichthyolith Issues, Special Publication 8, Yerevan, Armenia.
- Ginter M, Ivanov A. 1996. Relationships of *Phoebodus*. Mod Geol 20:263–274.
- Ginter M, Hairapetian V, Klug C. 2002. Famennian chondrichthyans from the shelves of North Gondwana. Acta Geol Pol 52:169–215.
- Gould SJ, Vrba ES. 1982. Exaptation—A missing term in the science of form. Paleobiology 8:4–15.
- Gross W. 1973. Kleinschuppen, Flossenstacheln und Zähne von Fischen aus Europäischen und Nordamerikanischen Bonebeds des Devons. Palaeontographica 142:51–155.
- Herold RC, Graver HT, Christner P. 1980. Immunohistochemical localization of amelogenins in enameloid of lower vertebrate teeth. Science 207:1357–1358.
- Iwai-Liao Y, Higashi Y, Tamada Y. 1992. Tooth tissues of certain sharks and lungfishes. Scanning Microsc 6:219–230.
- Janvier P. 1978. On the oldest known teleostome fish *Andeolepis hedei* Gross (Ludlow of Gotland) and the systematic position of the lophosteids. Proc Estonian Acad Sci Geol 27:88–95.
- Janvier P. 1996. Early vertebrates, Oxford Monographs on Geology and Geophysics 33. New York: Academic Press. 393 p.
- Johanson Z, Smith MM. 2003. Placoderm fishes, pharyngeal denticles, and the vertebrate dentition. J Morphol 257:289–307.
- Kemp NE. 1985. Ameloblastic secretion and calcification of the enamel layer in shark teeth. J Morphol 184:215–230.
- Long JA. 1986. New ischnacanthid acanthodians from the Early Devonian of Australia, with comments on acanthodian interrelationships. Zool J Linn Soc 87:321–229.
- Luer CA, Blum PC, Gilbert PW. 1990. Rate of tooth replacement in the nurse shark. *Ginglymostoma cirratum*. Copeia 1990:182–191.
- Lund R, Grogan ED. 1997. Relationships of the Chimaeriformes and the basal radiation of the Chondrichthyes. Rev Fish Biol Fisher 7:65–123.
- Maisey JG. 1980. An evaluation of jaw suspension in sharks. Am Mus Nov 2706:1–17.
- Maisey JG. 1984. Chondrichthyan phylogeny: A look at the evidence. J Vert Pal 4:359–371.
- Maisey JG. 1986. Heads and tails: A chordate phylogeny. Cladistics 2:201–256.
- Maisey JG. 2001. A primitive chondrichthyan braincase from the middle Devonian of Bolivia. In: Ahlberg PE, editor. Major Events in Early Vertebrate Evolution: Palaeontology, Phylogeny, Genetics and Development. London: Taylor & Francis. pp 263–288.
- Maisey JG, Naylor GJP, Ward DJ. 2004. Mesozoic elasmobranchs, neoselachian phylogeny and the rise of modern elasmobranch diversity. In: Arratia G, Tintori A, editors. Mesozoic fishes 3—Systematics, paleoenvironment and biodiversity. Munich: Pfeil. pp 17–56.
- Meinke DK. 1982. A histological and histochemical study of developing teeth in *Polypterus* (Pisces, *Actinopterygii*). Arch Oral Biol 27:197–206.
- Moss ML. 1967. Tooth replacement in the lemon shark, *Negaprion brevirostris*. In: Gilbert PW, Mathewson RF, Rall DP, editors. Sharks, Skates and Rays. Baltimore: Johns Hopkins. pp 319–329.
- Moss ML. 1977. Skeletal tissues in sharks. Am Zool 17:335–342.
- Moss SA. 1972. The feeding mechanisms of sharks of the family Carcharhinidae. J Zool Lond 167:423–436.
- Moss SA. 1977. Feeding mechanisms in sharks. Am Zool 17:355–364.
- Ørvig T. 1966. Histologic studies of ostracoderms, placoderms and fossil elasmobranchs, Part 2: On the dermal skeleton of two late Palaeozoic elasmobranchs. Ark Zool 19:1–39.
- Ørvig T. 1978. Microstructure and growth of the dermal skeleton in fossil actinopterygian fishes; Birgerids and Scanilepis. Zool Scr 7:33–56.
- Ørvig T. 1985. Histologic studies of ostracoderms, placoderms and fossil elasmobranchs, Part 2: Ptyctodontid tooth plates and their bearing on holocephalan ancestry: The condition of chimaerids. Zool Scr 14:55–79.

- Preuschoft H, Reif W-E, Müller WH. 1974. Funktionsanpassungen in form und struktur an haifischzähnen. *Z Anat Entwickl-Gesch* 143:315–344.
- Prostak KS, Skobe Z. 1988. Ultrastructure of odontogenic cells during enameloid matrix synthesis in tooth buds from an elasmobranch. *Raja erinacea*. *Am J Anat* 182:59–72.
- Prostak KS, Seifert P, Skobe Z. 1990. The effects of colchicine on the ultrastructure of odontogenic cells in the common skate. *Raja erinacea*. *Am J Anat* 189:77–91.
- Raff RA. 1996. *The Shape of Life: Genes, Development, and the Evolution of Animal Form*. Chicago: University of Chicago Press. 520 p.
- Reif W-E. 1973. Morphologie und Ultrastruktur des Hai-“Schmelzes”. *Zool Scr* 2:231–250.
- Reif W-E. 1977. Tooth enameloid as a taxonomic criterion, Part 1: A new euselachian shark from the Rhaetic-Liassic boundary. *N Jb Geol Paläont Mh* 1977:565–576.
- Reif W-E. 1978. Bending-resistant enameloid in carnivorous teleosts. *N Jb Geol Paläont Abh* 157:173–175.
- Reif W-E. 1979. Structural convergence between enameloid of actinopterygian teeth and of shark teeth. *Scan Electron Microsc* 1979:547–554.
- Reif W-E. 1982. Evolution of dermal skeleton and dentition in vertebrates: The odontode regulation theory. *Evol Biol* 15:287–368.
- Richter M, Smith MM. 1995. A microstructural study of the ganoine tissue of selected lower vertebrates. *Zool J Linn Soc* 114:173–212.
- Ripa LW, Gwinnett AJ, Guzman C, Legler D. 1972. Microstructural and microradiographic qualities of lemon shark enameloid. *Arch Oral Biol* 17:165–173.
- Risnes R. 1990. Shark tooth morphogenesis. An SEM and EDX analysis of enameloid and dentin development in various shark species. *J Biol Buccale* 18:237–248.
- Sansom IJ, Smith MM, Smith MP. 1996. Scales of thelodont and shark-like fishes from the Ordovician of Colorado. *Nature* 379:628–630.
- Sasagawa I. 1989. The fine structure of initial mineralisation during tooth development in the gummy shark. *Mustelus manazo*, Elasmobranchia. *J Anat* 164:175–187.
- Sasagawa I. 1997. Fine structure of the cap enameloid and of the dental epithelial cells during enameloid mineralisation and early maturation stages in the tilapia, a teleost. *J Anat* 190:589–600.
- Sasagawa I. 1999. Fine structure of the dental epithelial cells and the enameloid during the enameloid formation stages in an elasmobranch. *Heterodontus japonicus*. *Anat Embryol* 200:477–486.
- Sasagawa I. 2002. Mineralization patterns in elasmobranch fish. *Microsc Res Technol* 59:396–407.
- Satchell PG, Anderton X, Ryu OH, Luan X, Ortega AJ, Opamen R, Berman BJ, Witherspoon DE, Gutmann JL, Yamane A, Zeichner-David M, Spimmer JP, Shuler CF, Diekwisch TGH. 2002. Conservation and variation in enamel protein distribution during vertebrate tooth development. *J Exp Zool B Mol Dev Evol* 294:91–106.
- Schaeffer B. 1967. Comments on elasmobranch evolution. In: Gilbert PW, Matthewson RF, Rall DP, editors. *Sharks, Skates and Rays*. Baltimore: Johns Hopkins. pp 3–35.
- Schaeffer B, Williams M. 1977. Relationships of fossil and living elasmobranchs. *Am Zool* 17:293–302.
- Shellis RP. 1975. A histological and histochemical study of the matrices of enameloid and dentine in teleost fishes. *Arch Oral Biol* 20:183–187.
- Shellis RP, Miles AEW. 1974. Autoradiographic study of the formation of enameloid and dentine matrices in teleost fishes using tritiated amino acids. *P Roy Soc Lond B Bio* 185:51–72.
- Shellis RP, Miles AEW. 1976. Observations with the electron microscope on enameloid formation in the Common Eel (*Anguilla anguilla*; Teleostei). *P Roy Soc Lond B Biol* 194:253–269.
- Shirai S. 1992. *Squalean Phylogeny: A New Framework of “Squaloid Sharks” and Related Taxa*. Sapporo: Hokkaido University Press. 151 p.
- Shirai S. 1996. Phylogenetic interrelationships of neoselachians (Chondrichthyes: Euselachii). In: Stiassny MLJ, Parenti KR, Johnson GD, editors. *Interrelationships of Fishes*. San Diego: Academic Press. pp 9–34.
- Smith AB. 1994. *Systematics and the Fossil Record: Documenting Evolutionary Patterns*. Oxford: Blackwell Scientific. 223 p.
- Smith MM. 1992. Microstructure and evolution of enamel amongst osteichthyan fishes and early tetrapods. In: Smith P, Tchernov E, editors. *Structure, Function and Evolution of Teeth*. Tel Aviv: Freund Publishing House. pp 73–101. Proceedings of the 8th International Symposium on Dental Morphology.
- Smith MM. 1995. Heterochrony in the evolution of enamel in vertebrates. In: McNamara KJ, editor. *Evolutionary Change and Heterochrony*. Chichester: Wiley. pp 125–150.
- Smith MM. 2003. Vertebrate dentitions and the origin of jaws: When and how patterns evolved. *Evol Dev* 5:394–413.
- Smith MM, Hall BK. 1990. Development and evolutionary origins of vertebrate skeletogenic and odontogenic tissues. *Biol Rev* 65:277–373.
- Smith MM, Hall BK. 1993. A developmental model for evolution of the vertebrate exoskeleton and teeth: The role of cranial and trunk neural crest. *Evol Biol* 27:387–447.
- Smith MM, Johanson Z. 2003. Separate evolutionary origins of teeth from evidence in fossil jawed vertebrates. *Science* 299:1235–1236.
- Summers AP, Ketcham RA, Rowe T. 2004. Structure and function of the horn shark (*Heterodontus francisci*) cranium through ontogeny: Development of a hard prey specialist. *J Morphol* 260:1–12.
- Thies D. 1982. A neoselachii shark tooth from the Lower Triassic of the Kocaeli (= Bithynian) Peninsula, W Turkey. *N Jb Geol Paläont Mh* 1982:272–278.
- Thies D, Reif W-E. 1985. Phylogeny and evolutionary ecology of Mesozoic Neoselachii. *N Jb Geol Paläont Abh* 169:333–361.
- Williams ME. 1990. Feeding behavior in Cleveland Shale fishes. In: Boucrot AJ, editor. *Evolutionary Palaeobiology of Behavior and Coevolution*. Oxford: Elsevier. pp 273–287.
- Williams ME. 2001. Tooth retention in cladodont sharks: With a comparison between primitive grasping and swallowing, and modern cutting and gouging feeding mechanisms. *J Vert Pal* 21:214–226.
- Young GC. 1982. Devonian sharks from South-Eastern Australia and Antarctica. *Palaeontology* 25:817–843.
- Young GC. 1986. The relationships of placoderm fishes. *Zool J Linn Soc* 88:1–57.
- Zangerl R. 1973. Interrelationships of early chondrichthyans. In: Greenwood PH, Miles RS, Patterson C, editors. *Interrelationships of Fishes*. New York: Academic Press. pp 1–14.